IEEE Access
Multidisciplinary | Rapid Review | Open Access Journal

Received August 18, 2020, accepted September 1, 2020, date of publication September 11, 2020,
date of current version September 24, 2020.

Digital Object Identifier 10.1109/ACCESS.2020.3023552

Rate Control With Spatial Reuse for Wi-Fi 6 Dense Deployments

ALEXANDER KROTOV[1,2], (Member, IEEE), ANTON KIRYANOV[1,2], AND EVGENY KHOROV[1,3], (Senior Member, IEEE)

[1]Wireless Networks Laboratory, Institute for Information Transmission Problems of the Russian Academy of Sciences, 127051 Moscow, Russia
[2]Telecommunication Systems Laboratory, National Research Institute Higher School of Economics, 101000 Moscow, Russia
[3]Moscow Institute of Physics and Technology, 141701 Dolgoprudny, Russia

Corresponding author: Evgeny Khorov (e@khorov.ru)

This work was done at IITP RAS and supported by the Russian Science Foundation under Grant # 20-19-00788.

ABSTRACT To improve the performance of Wi-Fi networks in dense deployments, the recent IEEE 802.11ax standard introduces a palette of features improving spatial reuse. A key property of these features is dynamic changes in transmit power and the interference from the neighboring devices. The paper explains the basic operation of spatial reuse features and shows that their efficiency significantly depends on how the stations select appropriate modulation and coding schemes taking into account the variable transmission conditions. Nevertheless, the majority of existing studies in the literature leave this effect out of consideration, assuming an ideal rate control algorithm and obtaining wrong results. The paper fills this gap and presents a novel statistics-based rate control algorithm that selects modulation and coding schemes taking into account the effects induced by the recent spatial reuse features. With extensive simulation, it is shown that the algorithm significantly outperforms the existing rate control algorithms, providing up to 50% higher goodput and three times lower latencies.

INDEX TERMS Wi-Fi, 802.11ax, dense networks, spatial reuse, rate control, Thompson sampling, particle filter.

I. INTRODUCTION

Nowadays, Wi-Fi networks are densely deployed in offices, malls, airports, multi-apartment buildings. Although in these scenarios, the APs (access points) can be located every five or ten meters, the users may experience poor connection with low speeds and high losses caused by huge interference from neighboring devices even if the users are close to their AP. The technology that has been providing connectivity for decades degrades while the network density grows. That is why Cisco called interference a silent killer of Wi-Fi networks [1].

The recent 802.11ax, also known as Wi-Fi 6 [2], introduces a palette of methods that modify channel access to improve Wi-Fi performance in dense environments. Note that although the developers of 802.11ax desired to increase throughput at the user layer four times compared to 802.11ac, the real increase of the nominal data rates caused by new MCSs (modulation and coding schemes) is just 37%. At the same time, the more efficient channel usage shall achieve the rest. For that, 802.11ax defines data transmission with OFDMA (Orthogonal Frequency-Division Multiple Access). OFDMA allows using the best subchannels for wireless transmission prone to frequency-selective fading and interference, and many methods that improve spatial reuse.

Focusing on spatial reuse means the paradigm shift for the Wi-Fi community. From the very beginning, in Wi-Fi, advanced channel assess methods tried to forbid neighboring devices to access the channel during the ongoing transmissions. This paradigm was implemented in the RTS/CTS (Request-to-send/Clear-to-send) handshake of the first Wi-Fi standard, in MCCA (Mesh coordination function Coordinated Channel Access) of 802.11s that specifies mesh Wi-Fi networks, and HCCA TXOP (Hybrid coordination function Coordinated Channel Access Transmission Opportunity) Negotiation in 802.11aa [3]. The community considered similar approaches at the beginning of the 802.11ax development process. Still, finally, most of the approved features work inversely: during one transmission, they allow another one if it cannot corrupt the first one. As we explain in detail in Section II, such overlapping transmissions occur at lower powers. That is why at the receiver, the SINR (signal to

The associate editor coordinating the review of this manuscript and approving it for publication was Wei Liu.

interference plus noise ratio) for overlapping transmission is lower than for the usual ones. It means that the transmitter shall select a lower MCS for the overlapping transmissions to take into account the peculiarities of spatial reuse operation.

Unfortunately, the MCS selection (or how it is often called in Wi-Fi, ''rate control'') algorithms are outside the standard's scope. Although in the literature, there are plenty of rate control algorithms developed for legacy Wi-Fi networks [4]–[6], they do not perform correctly with the 802.11ax spatial reuse. Moreover, in the paper, we show that new spatial reuse features with popular rate control algorithms sometimes provide even negative gains. That is why the existing works on 802.11ax spatial reuse typically assume an ideal rate control, use constant MCS or even hide this issue [7]–[16]. At the same time, in 802.11ax, given the bandwidth, the slowest and the fastest MCS in a spatial stream differ ≈30 times. It means that the rate control algorithm has a significant impact on the overall network performance.

The contribution of the paper is threefold. First, we provide a brief introduction to the spatial reuse features that became maybe the most debatable part of the 802.11ax specification [2]. Second, we design a new rate control algorithm that can work in conjunction with the spatial reuse methods. The algorithm takes into account the peculiarities of 802.11ax spatial reuse, e.g., the highly variable SINRs. The algorithm makes decisions based on the gathered statistics on transmission successes and failures. So, it does not require any sounding information and can be used even for relatively rare data transmissions. Third, with extensive simulation, we show that the algorithm significantly outperforms the existing rate control algorithms, providing up to 50% higher goodput and up to three times lower latency. In contrast, the spatial reuse with the widely used Minstrel algorithm may even degrade the performance.

The rest of the paper is organized as follows. In Section II, we describe several approaches proposed in the IEEE 802.11ax amendment to increase the performance of dense Wi-Fi networks by improving spatial reuse. In Section III, we analyze various approaches for rate control design and overview of exiting solutions. Section IV describes the designed rate control algorithm. In Section V, we evaluate the performance of the designed rate control and compare it with others. Sections VI concludes the paper.

II. BRIEF DESCRIPTION OF SPATIAL REUSE IN 802.11ax

A. LEGACY CARRIER SENSE

Wi-Fi, including the recent Wi-Fi 6 [2] and Wi-Fi 7 [17] versions, uses a CSMA/CA (Carrier Sense Multiple Access with Collision avoidance) method with truncated binary exponential backoff. It means that before accessing the channel, a STA (station) initializes a backoff counter with a random value. When the channel is idle, the backoff counter is decremented every slot of 9 us (for 5 GHz bands). When the channel is busy, the STA suspends the backoff counter. The STA resumes backoff when the channel becomes idle again for at least the Arbitration Inter-Frame Space (AIFS). If the previous packet is not decoded correctly, this interframe space is extended by the time needed to transmit an acknowledgment frame. When the backoff counter reaches zero, and the channel is idle, the STA starts a frame exchange sequence called Transmission Opportunity (TXOP).

For many years, the Wi-Fi developers' strategy has been based on deferring transmission whenever there is even a small risk for the packets to collide. So, they have introduced many indicators that the channel is physically or virtually busy. A device has to consider the channel as busy if at least one of them indicates so. The main channel busy indicators are as follows.

- PD Packet Detect. When a STA detects a packet preamble, it considers the channel as busy for the packet duration signaled in the preamble. The STA must detect the packets if the signal strength is at least −82 dBm.[1] However, in real devices, this threshold is lower and depends on the quality of the receiver.
- ED Energy Detect. When a STA has not detected the preamble but detects an unknown signal at least 20 dB higher than the minimum sensitivity level, it considers the channel as busy for the duration of this signal.
- NAV Virtual Carrier Sense called Network Allocation Vector. The NAV can be considered as a counter indicating how long the channel will be virtually busy. It counts down uniformly until it reaches zero. When NAV is zero, the channel is idle. Otherwise, it is busy.

  When a STA transmits a frame, it indicates in the MAC (Medium Access Control) header of the frame the expected duration of the following frame sequence. Having received this frame, the neighboring STAs update their NAV with the indicated value if it exceeds the current NAV value. Otherwise, they do not change the NAV. If a STA has reserved more time than needed, it releases the remaining time by sending a CF-End frame. Having received this frame, the STAs reset their NAV timers.

B. 802.11ax FEATURES FOR SPATIAL REUSE

The described above framework works rather well in a spatially isolated Wi-Fi network, or a BSS (Basic Service Set) in terms of the 802.11 standard. If multiple BSSs operate in the same area at the same frequencies, a STA needs to defer its transmission whenever it receives a weak frame from the neighboring BSS (called Overlapped BSS, OBSS). Such an operation avoids spatial reuse and causes low overall throughput.

To improve spatial reuse in such scenarios, 802.11ax introduces many features based on the ability of the 802.11ax devices to distinguish packets sent from their BSS and OBSS [2].

[1] Hereinafter, the thresholds are given for the basic bandwidth of 20 MHz.

1) COLOR

Notably, 802.11ax devices can determine which BSS is the originator of an 802.11ax packet without decoding the entire packet. For that, each BSS has a pseudo-unique 6-bit long ID, called color, that is indicated in the 802.11ax packet preamble. The BSS colors are selected randomly by the APs (Access Points). So the colors of two neighboring BSSs may coincide. In such a case, the STAs notify the AP, which they are associated with, and the AP can start a procedure of changing its BSS color. Thanks to the BSS color, 802.11ax devices can quickly distinguish intra-BSS and inter-BSS frames. This ability can improve performance for both virtual and physical carrier sense.

2) TWO NAVs

In previous Wi-Fi standards, virtual carrier sense rules did not take into account the origin of the NAV. In dense networks, such behavior may be incorrect. Suppose an intra-BSS packet sets the NAV value at a STA. After that, the STA receives an inter-BSS CF-End, indicating that inter-BSS STA has no more frames to transmit and wants to terminate the TXOP, as described in Section II-A. The STA resets its NAV and considers the medium to be idle. So, the STA can start a transmission, which may collide with a transmission from a hidden intra-BSS STA. A similar situation may happen if the NAV set by an inter-BSS frame is reset by an intra-BSS CF-End. To prevent an inter-BSS CF-End from resetting the NAV set up by an intra-BSS frame, and vice versa, 802.11ax STAs support two NAVs. The first one is used for those transmissions that are recognized as intra-BSS. The second one, called Basic NAV, is used for inter-BSS frames and for those frames that have not been recognized as inter-BSS or intra-BSS, for example, for legacy ACK frames that contain an unknown address.

Note that a more complex situation, when an inter-BSS NAV is reset by a CF-End from another OBSS, has been considered by the IEEE 802.11ax developers, but introducing more than two NAVs was not approved because of high implementation complexity.

3) OBSS PD

802.11ax enhances the physical carrier sense by allowing the STAs to tune the PD threshold adaptively. A higher PD threshold means that the STA can ignore more ongoing transmissions. As typically in Wi-Fi networks, transmissions occur between an AP and associated STAs, ignoring intra-BSS transmissions has no sense. So, only inter-BSS transmissions may be ignored. That is why 802.11ax introduces a separate OBSS_PD threshold and applies it only for inter-BSS transmissions. When the OBSS_PD threshold is changed, the PD threshold used for intra-BSS frames always stays at the same −82 dBm level.

Accessing the channel during ongoing low-power inter-BSS frames interferes with these frames. IEEE 802.11ax makes this interference lower than −82 dBm, i.e., the legacy PD and, thus, the acceptable interference in the legacy networks. For that, the STA reduces the transmit power by at least X dB if it increases OBSS_PD by X dB. The increased level of PD cannot exceed −62 dBm, which is the ED threshold imposed by the regulatory limitations, see Fig. 1. Note that because of the channel reciprocity, such a simultaneous change in PD and transmit power changes the interference range of neighboring BSSs and virtually separates them, as shown in Fig. 2.

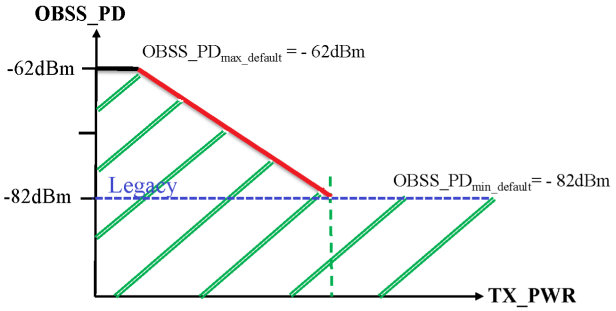

FIGURE 1. OBSS_PD and transmission power adjustment.

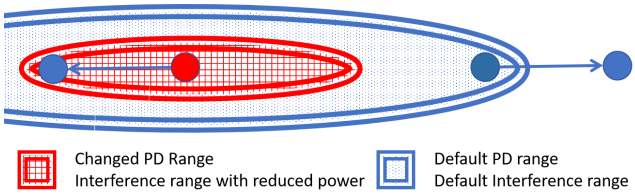

FIGURE 2. Virtual separation of neighboring BSSs.

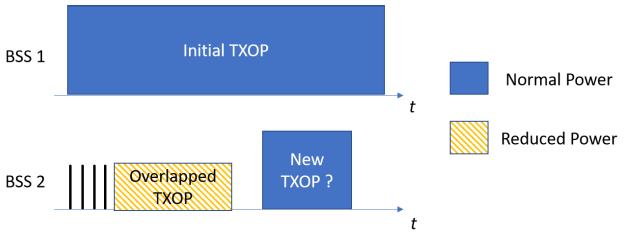

FIGURE 3. Overlapped TXOP during initial TXOP.

Consider a scenario with two BSSs. Let a STA from BSS 1 start a transmission, which we refer to as the *initial TXOP*, see Fig. 3. When a STA from BSS 2 detects an inter-BSS packet with the power lower than OBSS_PD, it can reset the channel state to idle before the end of the packet (i.e., the basic NAV timer is not invoked) and continue the backoff procedure to access the channel if no other conditions indicate that the channel is busy. Such conditions include intra-BSS NAV reserving the channel for other STA transmissions in the same BSS and unknown signals above the ED threshold, e.g., LTE networks operating in an unlicensed spectrum using the License Assisted Access technology.

When the backoff reaches zero, the STA can set up its own TXOP, which we refer to as *overlapped TXOP*. During the whole overlapped TXOP, the STA shall transmit with the reduced power, according to Fig. 1. The standard does not limit the duration of the overlapped TXOP obtained with the changed OBSS_PD, leaving many details implementation-dependent. For example, it is not specified if this TXOP can exceed the remaining duration of the initial TXOP. Also, the channel access rules after the overlapped TXOP are not specified. Finally, the standard does not indicate how often the STA can change its OBSS_PD.

To fill the gaps in the standard, let us analyze the peculiarities of the Wi-Fi channel access. If a STA has ignored the frame preamble and has not set up its NAV, only ED may indicate that that the channel is busy. ED indicates a busy channel only if the STA senses the signal stronger than -62 dBm. However, the OBSS PD operation is only allowed if the signal strength is below -62 dBm. Thus, if the overlapped TXOP is much shorter than the remaining part of the initial TXOP, and the STA tries to access the channel right after the overlapped TXOP, as shown in Fig. 3, it very likely finds the channel as idle. Thus, after the short transmission with the reduced power, the STA can access the channel again and transmit with the full power, which will damage the transmissions in the initial TXOP.

As a result, even if a STA finishes its TXOP earlier than the initial TXOP, it shall be forbidden to access the channel next time before the end of the initial TXOP. Thus, it makes no sense to make overlapped TXOP shorter than the initial TXOP. On the other hand, because of the reduced transmit power, it is hardly fruitful to make the overlapped TXOP longer than the initial TXOP. Lower transmit power leads to a low Signal-to-Noise Ratio (SNR), which reduces the possible data rate. Summing up, the STA should try to make the overlapped TXOP of the same duration as the initial TXOP. Although such a rule is not in the standard yet, it is expected that the vendors follow it because it significantly affects the performance.

As for the frequency of OBSS_PD changes, the STA can adjust the OBSS_PD value every time an inter-BSS transmission starts. Such frequent changes in OBSS_PD, and consequently, transmit power and interference complicate MCS selection (or, as it is often called in the papers on Wi-Fi, rate control), as we show in the paper.

Finally, ignoring neighboring transmissions does not always provide gains. Moreover, in some situations, it may increase the rate of transmission failures, for example, when two APs located far from each other transmit data to the STAs that are close to each other. The standard does not specify when power-based spatial reuse shall be used, and when not. However, it provides a tool to coordinate spatial reuse operation as follows.

4) SPATIAL REUSE GROUPS

The standard introduces SRGs (spatial reuse groups). Each SRG consists of several BSSs and has its own SRG OBSS_PD. A STA can try to start its own transmission during another one if it belongs to the same SRG, and the signal strength is below the corresponding SRG OBSS_PD. The remaining rules are similar to those for the non-SRG OBSS_PD, which is described above. The standard provides no recommendation on how to configure the SRGs, which opens the door for future research.

Whatever version of SR is used, with or without SRG, tuning sensitivity level and transmit power affect the MCS selections. The lack of solutions on this problem limits the value of numerous studies on SRG presented in the literature that assume perfect knowledge of the interference level, as we show in detail in Section III.

5) CARRIER SENSE WITH OFDMA

Note that in addition to CSMA/CA, in IEEE 802.11ax, the STAs may access the channel with OFDMA that is described in detail in [2]. However, in Wi-Fi networks, OFDMA is implemented in a per-packet mode and works upon CSMA/CA. Having accessed the channel with CSMA/CA, the AP can send a frame, various frequency parts of which are destined to different STAs. The AP can also send a Trigger frame that splits the channel into several frequency parts, called resource units (RUs), and allocate the RUs to the STAs for deterministic or random access. SIFS after the Trigger frame, the STAs respond with their transmissions. In the Trigger frame, the AP indicates whether the STA shall respond with a UL frame regardless of the busy/idle state of the channel, or it shall check if the channel is idle. The standard allows us to ignore the channel state only for short transmissions such as acknowledgment frames, which in legacy Wi-Fi are sent independently of the channel state if the frames are delivered. For long data transmission, the STAs need to perform clear channel assessment that includes ED and NAV. The PD criterion is not used because within a SIFS between the end of the Trigger frame and the beginning of the following uplink transmission, no preamble can be detected.[2] As for the NAVs, associated STAs take into account only basic NAV, but intra-BSS NAV is ignored. The standard allows us to ignore the intra-BSS NAV because the AP plays the role of a channel access coordinator. Thus, if it allows transmission in its BSS, no intra-BSS NAV shall prevent it. If the STA is not associated with the AP yet, it ignores the NAV if it was set by a transmission from the same AP that sends the Trigger frame.

6) PARAMETRIZED SPATIAL REUSE

With Trigger frames, an AP can explicitly indicate in a Trigger frame the acceptable level of interference for the following uplink OFDMA transmission. An OBSS STA can ignore this transmission, count down backoff, and access the channel during this transmission if the intended transmit power induces interference at the AP below the indicated

[2]In the 5 GHz band, the packet detection requires 20 to 25 us, while SIFS is 16 us.

acceptable level. This method is called Parametrized Spatial Reuse (PSR). Briefly speaking, it works as follows. For each 20 MHz part of an 80 MHz channel or each 40 MHz part of a 160 MHz channel, the AP encodes in the Trigger frames the sum $T+I$ of its transmit power T and the acceptable interference I. Having received this Trigger frame with receive power R, the OBSS STA calculates $T-R+I$, which is the maximal affordable power with which the OBSS STA can transmit during the uplink transmission that follows the Trigger frame to induce interference below I at the AP. Note that because of the channel reciprocity, $R-T$ is the path loss between the AP and the OBSS STA, which is the same for both directions.

Since the downlink traffic is typically heavier than the uplink one, in the paper, we focus on the methods fruitful for downlink transmissions.

III. RELATED WORKS

A. SPATIAL REUSE

Many papers study various approaches for spatial reuse in dense 802.11ax networks. However, most of them ignore the problem of rate control and the interaction between spatial reuse mechanisms and rate control algorithms.

One of the earliest spatial reuse algorithms proposed for 802.11ax, which may be considered as the first step towards OBSS PD, is the Dynamic Sensitivity Control [18], [19]. The idea of the algorithm is that each STA measures RSSI (Received Signal Strength Indicator) of beacons sent by the AP to which the STA is associated, and adjusts the sensitivity threshold as follows:

$$\text{Threshold} = \text{Average RSSI} - \text{Margin}, \tag{1}$$

where Margin is a positive value that takes into account channel quality fluctuations. This algorithm leads to unfairness and allows increasing spatial reuse only for uplink transmissions. As shown in [20], such issues can be solved by adopting the *constant product rule*: the product of the sensitivity threshold and transmission power in absolute values shall remain constant for all transmitters. It is exactly the rule used by the OBSS PD spatial reuse mechanism in IEEE 802.11ax, see Fig. 1: except for the border values, the sum of the sensitivity threshold and the transmission power expressed in dB is constant.

In [14], the Dynamic Sensitivity Control mechanism is analyzed using the methods of stochastic geometry. In [21], [22] the authors study how to choose the optimal sensitivity threshold and derive a closed-form expression for the threshold that maximizes throughput. However, to make the problem tractable, these papers assume that only one MCS is used and, consequently, consider only one fixed target SINR.

In [13], a heuristic algorithm is proposed to choose the sensitivity threshold using a centralized controller. Evaluation is performed using a custom network simulator developed in C++. A rate control algorithm is not modeled, and the MCS is selected according to the table mapping 802.11a MCSs to corresponding SINR thresholds.

In [8], an 802.11ax network using the OBSS PD mechanism is modeled using the Komondor discrete-event simulator [15], which has lower computation complexity than existing simulators such as NS-3 [23] at the cost of omitting rate control model and oversimplified PHY and MAC operation.

In [16], the authors propose a new channel access mechanism for 802.11ax that improves spatial reuse in dense deployments. The study is carried out with Matlab. However, the authors again consider an ideal rate control algorithm that selects an MCS that maximizes throughput for given channel conditions.

Summing up, the existing study of spatial reuse algorithms either do not consider the ability of the Wi-Fi devices to adaptively select an appropriate MCS or consider an ideal behavior. We believe that such oversimplification of Wi-Fi operation is done because the rate control algorithms widely used in the previous versions of Wi-Fi work wrong when combined with the OBSS PD mechanism. For confirmation, see the numerical results in Section V.

B. RATE CONTROL ALGORITHMS

Existing rate control algorithms can be categorized into two groups — sampling-based and measurement-based. To make a decision, sampling-based mechanisms use statistics about successes and failures for each MCS, while measurement-based mechanisms rely on explicit channel quality measurements.

1) MEASUREMENT-BASED ALGORITHMS

In measurement-based solutions, the devices typically use RSSI or SNR (Signal-to-Noise Ratio) to estimate the channel quality. Unfortunately, RSSI does not always correlate with the packet error rate and cannot reveal frequency-selective fading. Such algorithms are widely used in cellular networks operating in a licensed spectrum with predictable interference. For example, in LTE networks, the user equipments regularly feedback to a base station so-called CQI (Channel Quality Indicator). CQI indicates the quality of each 2–3 MHz frequency subband. Based on this feedback, the base station selects the best parts of the bandwidth for transmission and an appropriate MCS. Notably, later, the selected MCS is adjusted based on the positive and negative acknowledgments of data delivery.

In Wi-Fi, the STAs usually use random channel access. So the exact transmission time is unknown, and the channel quality feedback is not frequent and precise. There are several measurement-based rate control mechanisms for Wi-Fi, e.g., RBAR (Receiver-Based Auto Rate) [24], SampleLite [25]. First, some of them require changing the IEEE 802.11 protocol. Second, the noise in the unlicensed spectrum and the presence of hidden STAs badly influence their performance [26]. Because of the mentioned facts, sampling-based rate control mechanisms were historically used in Wi-Fi. In this paper, we focus on this group of solutions.

2) SAMPLING-BASED ALGORITHMS

Sampling-based approaches rely on statistics about successful and failed transmissions. Classical sampling-based solutions include ARF (Auto Rate Fallback) [27], AARF (Adaptive ARF) [28], SampleRate [29]. Another rate control algorithm, probably the most widespread one for Wi-Fi networks, is Minstrel and its extension Minstrel-HT [30] for high throughput Wi-Fi, i.e., 802.11n/ac.[3] Each of these empirical solutions defines how to adaptively change the MCS, including testing the available MCSs.

Besides pure empirical decisions, many algorithms solve mathematical problems. In [31], [32], the authors show how to use a MAB (Multi-Armed Bandit) approach to select an appropriate rate. Specifically, each MCS represents an arm. A product of nominal MCS rate and the transmission success probability at a given MCS is the arm reward. Classical solutions to the MAB problem are ε-greedy, UCB (Upper Confidence Bound), and TS (Thompson Sampling) algorithms.

The simplest approach is ε-greedy. Based on the accumulated statistics for different MCSs, the algorithm chooses an MCS with the maximum expected reward estimated as the sum of empirical mean rewards. However, with a small probability ε, the algorithm tries to find a better decision and chooses a random MCS to get more statistics on it. A major drawback of this algorithm is a linear regret. ε percent of the time is always wasted for testing suboptimal arms.

The UCB algorithms generally represent a frequentist approach to the MAB problem, which means they operate without an assumption on the prior reward distribution. They provide an optimistic assessment of rewards based on obtained statistics. An assessment for the arm is the sum of empirical mean rewards and so-called *confidence width* that encourages exploration of unknown arms. The improvement of classical UCB algorithm [33], namely Kullback-Leibler UCB (KL-UCB) algorithm [34], provides uniformly better regret bound than UCB.

The next approach to the MAB problem is Bayesian one that is used in the TS algorithms [35]. Let us consider a Bernoulli bandit with K arms, each corresponding to a transmission with a certain MCS. Each arm produces either a successful transmission or a failure. In the case of success, the reward equals the nominal MCS rate. The success probabilities $p_i, i \in \overline{1, K}$ are beta-distributed. After each observation, TS updates posterior distributions according to Bayes rule. To make a decision and estimate a potential reward, TS samples success probabilities p_i from posterior distributions and multiplies them by nominals MCS rates. When an action (i.e., MCS) is insufficiently explored, the posterior distribution is wide, and the probability of choosing this action is high.

TS is very complicated for analytical investigation. Although it has a long history, only recently in [36], the authors proved the asymptotic optimality of the TS algorithm for Bernoulli rewards. In practice, TS shows even better results than KL-UCB [37]. In [37], the authors also proposed a Unimodal TS (UTS) algorithm that utilized the unimodality property. Notably, UTS outperforms KL-UCB.

There are several modifications to the rate selection problem. In [38], the authors applied TS to optimize rate selection in the presence of latency constraints. In [39], the algorithm for the random channel with n states is developed and compared to TS-based algorithms via simulation.

C. REFERENCE ALGORITHMS

We compare the performance of the algorithm designed in Section IV with two reference ones. The first one is a widely used rate control algorithm, namely Minstrel. The second one is our straightforward extension of the Thompson sampling approach with the smoothing window to take into account the fluctuations of the wireless channel conditions and the interference and power levels.

1) MINSTREL

Minstrel has been originally developed in the MadWifi (Multiband Atheros Driver for Wi-Fi) project [40]. It is a sampling-based reference rate control algorithm. For each rate, Minstrel collects statistics of transmission attempts and evaluates actual throughput as success probability multiplied by packet payload and divided by packet transmission time.

Before transmitting a new frame, Minstrel determines the sequence of the following rates:

1) the best throughput rate,
2) the second-best throughput rate,
3) the highest success probability rate,
4) the lowest rate.

For each of these rates, Minstrel also defines the maximal number of transmission attempts that can be used successively. E.g., if k_1 transmission attempts at the best throughput rate turn out unsuccessful, then up to k_2 transmission attempts at the second-best throughput rate will be made. The maximum number of transmission attempts for each rate is chosen so that the trials' duration is limited by some value.

Besides, by default, 10% of the time, Minstrel operates in a ''look around'' mode and tries random rates. For that, the second-best throughput rate is replaced by a randomly selected rate. If a randomly selected rate exceeds the best throughput rate, then the randomly selected rate comes first.

A variant of the Minstrel algorithm called Minstrel-HT (High Throughput), which supports 802.11ac rates, is implemented in NS-3. We have further extended it to support 802.11ax rates.

2) THOMPSON SAMPLING

The second algorithm is based on the TS approach that works as follows. We suppose that for a given MCS (i.e., the transmission rate r_j), the number of successful transmissions follows the binomial distribution with unknown success probability q_j. To estimate the value of q_j given statistics

[3] In the paper, we use it as a reference one and describe in detail in Section V together with the other reference solutions.

of transmission successes, we take the beta distribution [41] with parameters $(1+\alpha_j, 1+\beta_j)$ as the conjugate prior, where α_j and β_j are the numbers of successful and unsuccessful transmissions for MCS j, correspondingly.

At the very beginning, $\alpha_j = \beta_j = 0, \forall j$, and thus for all MCSs, the success probability is distributed equally and uniformly. Then, α_j is incremented with every successful transmission, and β_j is incremented with every failure.

Every time we need a value for q_j, we sample it from the following beta distribution:

$$p(q_j) = \frac{q_j^{\alpha}(1-q_j)^{\beta}}{\mathrm{B}(\alpha_j, \beta_j)},$$

where $\mathrm{B}(\alpha_j, \beta_j)$ is the Beta function acting as a normalizing constant.

Thompson sampling-based rate control selects an MCS $\hat{j}$:

$$\hat{j} = \arg\max_j q_j r_j. \tag{2}$$

We improve the Thompson sampling approach by taking into account that the channel quality may change with time. Specifically, we use exponential smoothing after each transmission attempt:

$$\alpha_j(t) = \begin{cases} \alpha_j(t-\Delta t)\cdot e^{\frac{-\Delta t}{w}} + 1, & \text{in case of success} \\ \alpha_j(t-\Delta t)\cdot e^{\frac{-\Delta t}{w}}, & \text{otherwise,} \end{cases}$$

where $\alpha_j(t)$ is an estimation for the number of successful transmissions at the moment t, Δt is a time interval between the previous smoothing and the current smoothing (Δt is not a constant), w is the exponential window. $\beta_j(t)$ is smoothed similarly.

IV. POWER-AWARE RATE CONTROL BASED ON PARTICLE FILTER

The algorithms mentioned in Section III show relatively high performance under fixed transmission power and constant interference. However, to allow spatial reuse in dense deployment, the 802.11ax amendment describes new features under which a STA decreases its transmit power and sends data during another ongoing transmission. Choosing an MCS without taking into account changes in power and interference causes packet drops and performance degradation.

That is why, in this paper, we design a rate control algorithm that estimates the state of the channel, taking into account the peculiarities of the spatial reuse operation. The algorithm selects an MCS to maximize the goodput, i.e., the amount of delivered data within a time unit, for saturated links, and to minimize the data delivery delay for the non-saturated links.

Sampling rate control algorithms usually parameterize channel in n-dimensional space where n is the number of possible rates/MCSs. However, it is not obvious how to apply statistics obtained for transmissions with one power and interference level to make a decision for transmission with another power level. That is why, in this paper, we propose to change the channel parameterization paradigm. Instead of estimating the success probability for each transmission rate, we propose to parameterize the channel with a single variable reflecting interference and noise level. It allows us sampling the channel in one-dimensional space irrespective of the used transmit power level.

We implement this idea in a Power-aware Rate Control algorithm based on the Particle Filter (PF) [42]. For shortness, we refer to it as the PF algorithm.

For convenience, we split the PF algorithm into two logical parts, namely, (i) channel estimation and (ii) MCS selection. To estimate the channel quality, we use a particle filter when obtaining the probability distribution of the channel conditions, i.e., SINR. Then, having the distribution, we select the optimal MCS using the Thompson sampling approach described above.

A. CHANNEL ESTIMATION

Existing rate control algorithms based on the multi-armed bandit approach usually parameterize the channel as follows. For each MCS, they estimate success probability based on the number of successful and unsuccessful transmissions. Each time new statistics appear, they update the posterior distributions of success probabilities. To get the channel estimation, these probabilities are sampled from posterior beta distributions corresponding to each MCS. However, this approach is only feasible if the success probabilities for different MCSs are independent [39]. Otherwise, the complexity of sampling from multi-dimensional joint distribution grows exponentially as the number of dimensions increases.

To reduce the number of dimensions, we propose to describe the channel with a single parameter

$$\theta = \gamma / P_{\mathrm{tx}}, \tag{3}$$

or if we express all values in the logarithmic scale:

$$\theta = \gamma - P_{\mathrm{tx}}[dBm],$$

where γ is SINR and P_{tx} is the transmit power. Note that θ does not depend on the transmit power, as when the transmission power is changed, SINR is changed by the same amount in dB.

To estimate the posterior distribution of θ, we use a particle filter. Each particle (i.e., each sample) i is described by its position θ_i and probability p_i to be sampled from the distribution. We initialize the particle filter with N equidistant particles located at the range of the possible values of θ, each having a probability of $1/N$. For example, if SINR is between 0 dB and 30 dB for the transmit power of 20 dBm, and $N = 31$, the initial positions of the particles are: $-20, -19, \ldots, 9, 10$ dBm.

The properties of a particle, i.e., its position and probability, are updated according to specific measurement and prediction rules.

First, let us consider the measurement rule. Each transmission attempt represents a new observation (r, s), where r is the used transmission rate, $s \in \{0, 1\}$ is the result of the transmission (one in case of success, and zero otherwise).

We use the observation to recalculate p_i for each particle i as follows:

$$p_i^{(new)} = p_i^{(old)} \cdot P(s|r,\gamma)(1-P_c), \quad \text{if } s=1,$$

and

$$p_i^{(new)} = p_i^{(old)} \cdot (1-P(s|r,\gamma)(1-P_c)), \quad \text{if } s=0.$$

γ is the value corresponding to θ_i and used transmission power, $P(s|r,\gamma)$ is the conditional probability of successful (if $s=1$) or unsuccessful (if $s=0$) packet transmission attempt provided that the transmission rate is r and SINR is γ. $P(s|r,\gamma)$ is estimated from the known dependencies of transmission success probability on SINR for the given set of MCSs and the packet size, see Fig. 4 [43]. P_c represents the probability of unsuccessful packet transmission attempts because of CSMA/CA collision between nearby STAs. It happens when at least two STAs choose the same CSMA/CA backoff value. The value of P_c can be estimated as $1/CW$, where CW is the current size of the CSMA/CA contention window.

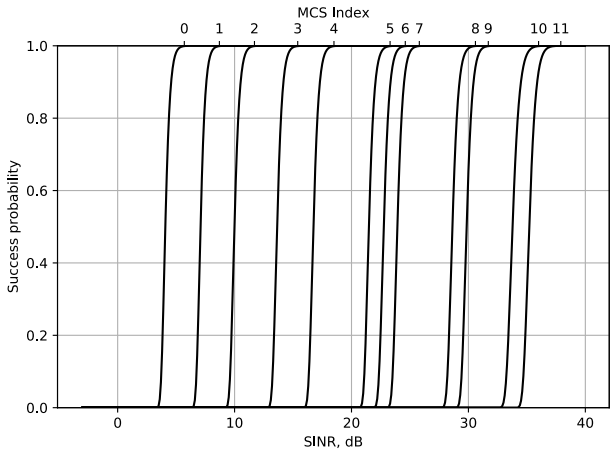

FIGURE 4. Success probability for each 802.11ax MCS and the MPDU size of 1500 B as a function of SINR [43].

Now, consider the prediction stage. Before sampling from the particle filter, we perform a prediction with preceding resampling, if necessary. First, we normalize weights, so $\sum_i p_i = 1$. Then, we estimate effective sample size $\frac{1}{\sum_i (p_i)^2}$. If it is less than $\frac{N}{2}$, we perform resampling: we sample the current θ distribution N times and thus get N new points. Each particle is again assigned with a probability of $1/N$. Resampling is necessary to eliminate many particles having close to zero probabilities without influencing estimated distribution.

After weight normalization and possible resampling, we apply prediction. Each particle is shifted according to the Wiener process. At the time t, each θ_i is updated as

$$\theta_i^{(new)} = \theta_i^{(old)} + W,$$

where $W \sim N(0, \eta\Delta t)$ is a normally distributed random variable with the average of zero and the variance $\eta\Delta t$. η is a parameter controlling the speed of SINR change, Δt is the time interval since the previous prediction update. The prediction step allows taking into account channel variations due to mobility, fading, etc.

After prediction, we sample a particle from the distribution p_i and obtain the corresponding value of θ. Then we select an MCS as described in the next section.

B. MCS SELECTION

We select an MCS based on the channel quality described by SINR value using the Thompson Sampling approach. Since we parameterized the channel with θ, we sample θ from the distribution and calculate expected SINR value according to (3).

For each MCS j that yields the nominal data rate r_j, we know the probability $P(1|r_j,\gamma)$ of a successful packet transmission. In order to maximize the expected rate, given the SINR value γ, the rate control algorithm selects MCS $\hat{j}$:

$$\hat{j} = \arg\max_j P(1|r_j,\gamma) r_j. \tag{4}$$

C. BSS COLOR USAGE

As described in Section II, to increase the flexibility of the spatial reuse operation, IEEE 802.11ax uses a BSS color included in a PHY header. Since this field can be decoded even before the whole packet is received, the receiver can make some decisions as soon as the BSS Color is sent over the air, e.g., the receiver can stop the frame reception and begin its own transmission. Since the interference from various OBSSs can vary significantly, we utilize a separate particle filter for each BSS color value.

V. PERFORMANCE EVALUATION

Let us evaluate the proposed algorithm with the NS-3 simulation platform, which is nowadays widely used for system-level performance evaluation [23]. We use the latest available NS-3 version in which the necessity for our investigations 802.11ax functionality is implemented. We also implemented the proposed rate control algorithms and evaluation scenarios. The main simulation parameters common for all considered scenarios are listed in Table 1. We consider three scenarios. In the first scenario, the simplest, unrealistic, but very tractable one, we evaluate the potential throughput gains of the designed algorithm, as well as the dependence of the gain on the channel quality fluctuation. In the second one, with two links that belong to different BSSs (see Fig. 8), we evaluate how the gain depends on the distances and attenuation between the nodes. In the last one, we model a dense Wi-Fi network in a huge multi-apartment building inspired by the IEEE simulation scenario document [44].

1) TRANSMISSION POWER CHANGE

In the first experiment, we consider a single Wi-Fi link between STAs A and B with the full-buffer traffic.

TABLE 1. Common simulation parameters.

Parameter	Value
Transport protocol	UDP
Channel model	[44]
Default AP TX power	21 dBm
Default STA TX power	21 dBm
Channel width	80 MHz
PD threshold	−82 dBm
ED threshold	−62 dBm
Attenuation on walls	10 dB
Frame capture margin	5 dB
$OBSS\_PD_{min}$	−82 dBm
$OBSS\_PD_{max}$	−62 dBm
Packet size	1500 bytes
A-MSDU aggregation	Disabled
A-MPDU aggregation	Enabled
Guard interval	3200 ns

The distance between STAs is ten meters. From time to time, STA A decreases its transmit power by Δ dB, and then increases it by the same amount, which models frequent SR operation. The interval between each change follows the exponential distribution with mean $1/\lambda$.

We compare the performance of the proposed PF rate control algorithm with the two reference algorithms: TS and Minstrel, described in Section III-C. To be fair, we consider various values of the exponential window w ranges from 0.001 to 1 second for the TS algorithm.

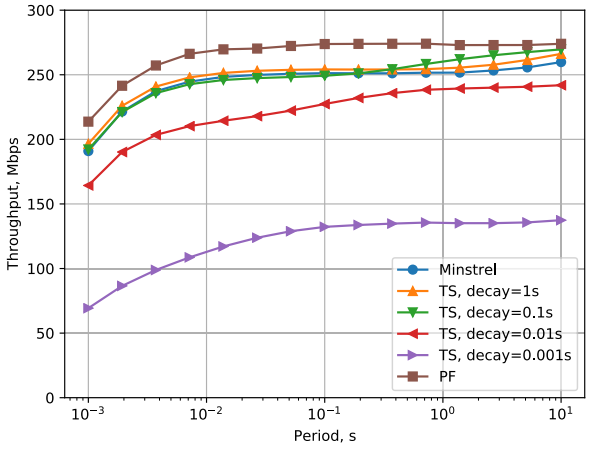

FIGURE 5. The dependence of link throughput on $1/\lambda$ for $\Delta = 5$ dB.

Figures 5–7 show the dependency of the link throughput on $1/\lambda$ for $\Delta = 5, 10, 15$ dB. For a small value of $\Delta = 5$ dB, all the considered solutions except for TS with small values of the exponential window show similar performance. For higher values of $\Delta = 10, 15$ dB PF outperforms all the other solutions for almost all values of λ. We can notice that for the TS algorithm, the highest throughput is achieved with different values of w for various values of λ. Taking into account these results, below, we set $w = 1$ s as it shows reasonable performance for a wide range of λ.

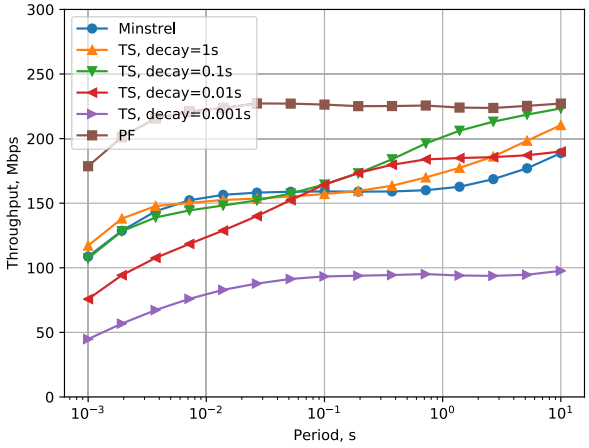

FIGURE 6. The dependence of link throughput on $1/\lambda$ for $\Delta = 10$ dB.

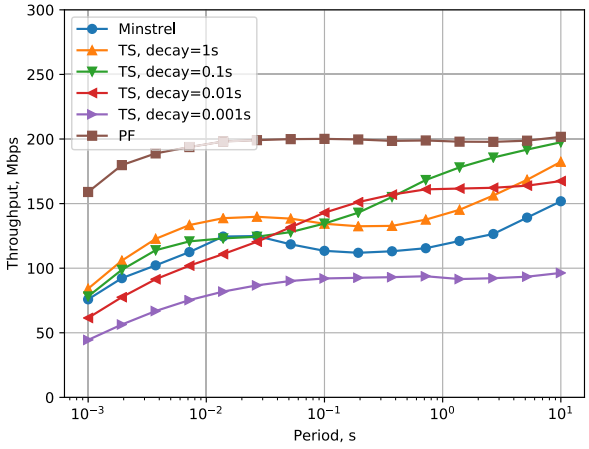

FIGURE 7. The dependence of link throughput on $1/\lambda$ for $\Delta = 15$ dB.

2) TWO LINKS SYMMETRIC SCENARIO

In this section, we show results for the set of experiments for two overlapped BSSs case, Fig. 8. In comparison with the previous section, we replace full-buffer traffic with a non-saturated one with a fixed bitrate. We vary the link range r, the distance d, and the load L at each link. Unless explicitly stated, in this set of experiments, $r = 5$ m, $d = 60$ m, $L = 200$ Mbps.

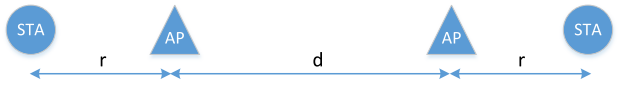

FIGURE 8. Two links symmetric scenario.

We compare the legacy behavior of Minstrel and TS rate control algorithms, i.e., when no OBSS PD spatial reuse is activated, with PF, TS, and Minstrel solutions under the enabled spatial reuse operation. Since the network is not

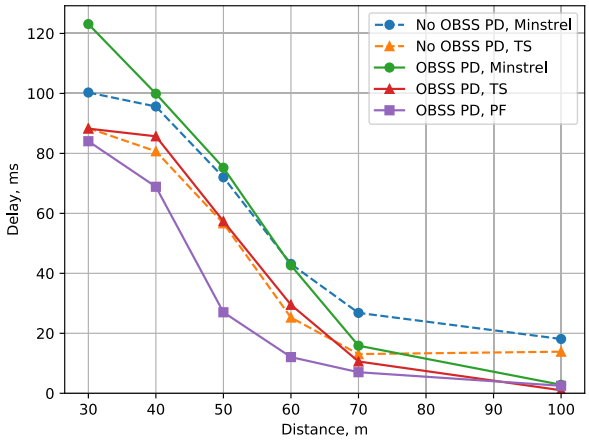

FIGURE 9. The dependence of delay on distance between BSS.

congested, we consider the average packet delay as a performance index.

First of all, let us study the efficiency of the designed algorithm when we vary the distance between two APs from 30 m to 100 m, see Fig. 9. Note that enabling OBSS PD spatial reuse with any reference rate control algorithms (Minstrel or TS) may even worsen the performance. It happens for small distances where interference between the APs is high, and an efficient rate control decision for simultaneous transmissions is extremely important. For large distances where the interference between the APs is small enough, the usage of OBSS PD spatial reuse significantly decreases the average packet delay irrespectively of implemented rate control. For all considered distances, the proposed PF algorithm shows the smallest packet delay, decreasing it up to two times compared with the best of the other solutions.

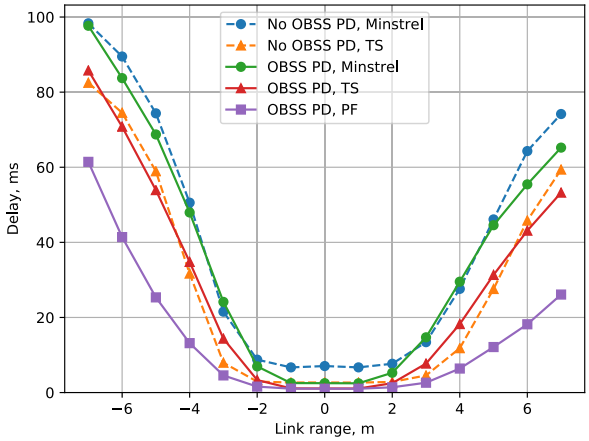

FIGURE 10. The dependence of delay on the distance between AP and STA.

In the next experiment, we vary the link range, i.e., the distance between the AP and the STA in both BSSs, Fig. 10. A positive link range means that APs are located between STAs, while a negative link range means that the STAs are located between the APs. For negative link ranges, the performance is worse than for the positive ones because the STAs become closer to the alien APs and experience stronger interference. Note that using the TS rate control algorithm together with OBSS PD spatial reuse decreases the performance again because TS does not expect changes in the TX power. Thus, sometimes it makes erroneous decisions. The proposed PF rate control outperforms all the other considered solutions decreasing the average packet up to two times again.

In the last experiment of this set, we vary the load at both links, Fig. 11. For a very light load, all the solutions show similar reasonable performance where the average packet delay does not exceed 5 ms. Notably, for light loads, the reference rate control algorithms, namely Minstrel and TS with no OBSS PD spatial reuse, outperform the corresponding ones with OBSS PD spatial reuse. It confirms our previous findings that it is better not to use the spatial reuse option than to use it with an inappropriate rate control solution. However, for a larger load, small gain thanks to the OBSS PD spatial reuse is yet achieved. The PF rate control algorithm designed in this paper decreases the average packet delay up to two – four times for middle and large load with only a tiny performance loss for a light load.

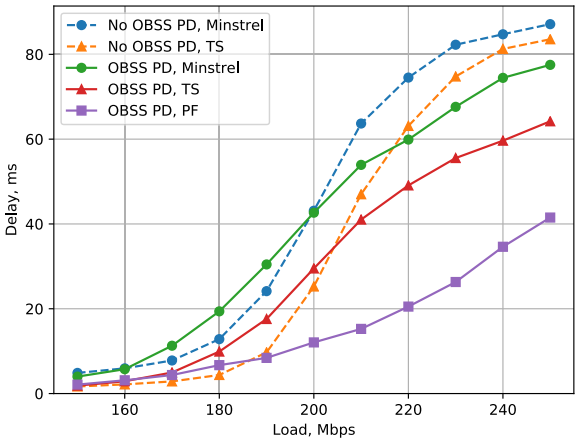

FIGURE 11. The dependence of delay on the load.

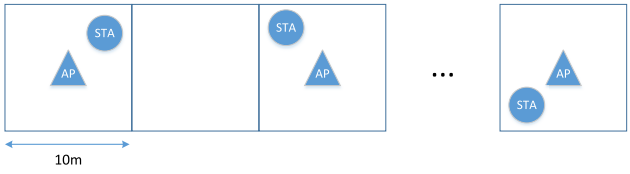

FIGURE 12. Residential building scenario.

3) RESIDENTIAL BUILDING SCENARIO

Finally, we consider a complicated scenario with several overlapped BSSs located in a residential building, Fig. 12. We model a single floor of a building where n apartments are located in a line. Each apartment is ten by ten meters. The AP is placed in the center of the room, and a Wi-Fi

client STA is placed in the room randomly. We suppose that the APs from neighboring apartments operate in different frequency channels and, thus, interfering APs are located in every other apartment (in our case, they have odd indexes). When interfering APs are separated by more than one apartment, the observed effect will be similar but less pronounced.

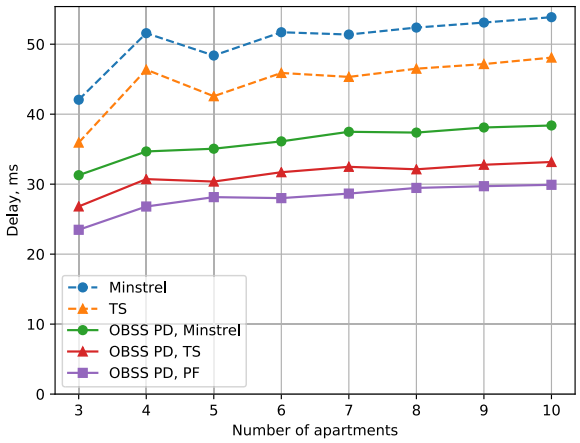

FIGURE 13. Results for the residential building.

Fig. 13 shows how the average packet delay depends on the building size, i.e., on the number of active rooms in which the APs operate on the same frequency channel. Here we find out that all the solutions with enabled OBSS PD spatial reuse are better than solutions without spatial reuse. The PF rate control algorithm shows the best results, which remain almost the same as the size of the building increases.

VI. CONCLUSION

In this paper, we consider the transmission rate selection problem in modern Wi-Fi networks. According to new spatial reuse algorithms proposed in the latest IEEE 802.11ax amendment, the STAs can modify their transmission power in order to enable simultaneous transmissions. Since legacy rate control algorithms are unaware of this capability, they often fail to choose an optimal transmission rate, which degrades network performance.

In this article, we proposed a novel rate control algorithm for 802.11ax Wi-Fi networks. Based on statistics of successful packet transmissions, the algorithm estimates channel quality irrespectively of transmission power using a particle filter approach. We implemented the designed PF rate control algorithm in a widely known NS-3 simulation environment and performed extensive performance evaluations in several scenarios. We found that the proposed PF solution significantly outperforms other considered rate control algorithms, increases throughput by up to 50%, and reduces the latency over twice.

Although the proposed algorithm can be used for MU-MIMO and OFDMA transmission, in future work we plan to take into account sounding feedback for when selecting an MCS for such multi-user transmissions.

REFERENCES

[1] Cisco. *Wireless High Client Density Design Guide*. Accessed: Sep. 1, 2020. [Online]. Available: https://www.cisco.com/c/en/us/td/docs/wireless/controller/technotes/8-7/b_wireless_high_client_density_design_guide.html

[2] E. Khorov, A. Kiryanov, A. Lyakhov, and G. Bianchi, "A tutorial on IEEE 802.11ax high efficiency WLANs," *IEEE Commun. Surveys Tuts.*, vol. 21, no. 1, pp. 197–216, 1st Quart., 2019.

[3] E. Khorov, A. Lyakhov, A. Ivanov, and I. F. Akyildiz, "Modeling of real-time multimedia streaming in Wi-Fi networks with periodic reservations," *IEEE Access*, vol. 8, pp. 55633–55653, 2020.

[4] W. Yin, P. Hu, J. Indulska, M. Portmann, and Y. Mao, "MAC-layer rate control for 802.11 networks: A survey," *Wireless Netw.*, vol. 26, pp. 3793–3830, 2020.

[5] S. Biaz and S. Wu, "Rate adaptation algorithms for IEEE 802.11 networks: A survey and comparison," in *Proc. IEEE Symp. Comput. Commun.*, Jul. 2008, pp. 130–136.

[6] M. A. Gawas and R. Tambi, "Data rate adaptation algorithms survey for IEEE 802.11 networks," in *Proc. Int. Conf. Current Trends Comput., Electr., Electron. Commun. (CTCEEC)*, Sep. 2017, pp. 926–932.

[7] I. Selinis, K. Katsaros, S. Vahid, and R. Tafazolli, "Control OBSS/PD sensitivity threshold for IEEE 802.11ax BSS color," in *Proc. IEEE 29th Annu. Int. Symp. Pers., Indoor Mobile Radio Commun. (PIMRC)*, Sep. 2018, pp. 1–7.

[8] F. Wilhelmi, S. Barrachina-Munoz, and B. Bellalta, "On the performance of the spatial reuse operation in IEEE 802.11ax WLANs," in *Proc. IEEE Conf. Standards Commun. Netw. (CSCN)*, Oct. 2019, pp. 1–6.

[9] Y. Kim, G. Kim, T. Kim, and W. Choi, "Transmission opportunity-based distributed OBSS/PD determination method in IEEE 802.11ax networks," in *Proc. Int. Conf. Artif. Intell. Inf. Commun. (ICAIIC)*, Feb. 2020, pp. 469–471.

[10] T. Ropitault and N. Golmie, "ETP algorithm: Increasing spatial reuse in wireless LANs dense environment using ETX," in *Proc. IEEE 28th Annu. Int. Symp. Pers., Indoor, Mobile Radio Commun. (PIMRC)*, Oct. 2017, pp. 1–7.

[11] N. Sepic, E. Kocan, and M. Pejanovic-Djurisic, "Evaluating spatial reuse in 802.11ax networks with interference threshold adjustment," in *Proc. 24th Int. Conf. Inf. Technol. (IT)*, Feb. 2020, pp. 1–4.

[12] I. Selinis, K. Katsaros, S. Vahid, and R. Tafazolli, "Exploiting the capture effect on DSC and BSS color in dense IEEE 802.11ax deployments," in *Proc. Workshop Ns-3 WNS3*, 2017, pp. 47–54.

[13] Y. Wen, H. Fujita, and D. Kimura, "Throughput-aware dynamic sensitivity control algorithm for next generation WLAN system," in *Proc. IEEE 28th Annu. Int. Symp. Pers., Indoor, Mobile Radio Commun. (PIMRC)*, Oct. 2017, pp. 1–7.

[14] A. Aijaz and P. Kulkarni, "On performance evaluation of dynamic sensitivity control techniques in next-generation WLANs," *IEEE Syst. J.*, vol. 13, no. 2, pp. 1324–1327, Jun. 2019.

[15] S. Barrachina-Munoz, F. Wilhelmi, I. Selinis, and B. Bellalta, "Komondor: A wireless network simulator for next-generation high-density WLANs," in *Proc. Wireless Days (WD)*, Apr. 2019, pp. 1–8.

[16] A. Valkanis, A. Iossifides, P. Chatzimisios, M. Angelopoulos, and V. Katos, "IEEE 802.11ax spatial reuse improvement: An interference-based channel-access algorithm," *IEEE Veh. Technol. Mag.*, vol. 14, no. 2, pp. 78–84, Jun. 2019.

[17] E. Khorov, I. Levitsky, and I. F. Akyildiz, "Current status and directions of IEEE 802.11be, the future Wi-Fi 7," *IEEE Access*, vol. 8, pp. 88664–88688, 2020.

[18] M. S. Afaqui, E. Garcia-Villegas, E. Lopez-Aguilera, G. Smith, and D. Camps, "Evaluation of dynamic sensitivity control algorithm for IEEE 802.11ax," in *Proc. IEEE Wireless Commun. Netw. Conf. (WCNC)*, Mar. 2015, pp. 1060–1065.

[19] M. S. Afaqui, E. Garcia-Villegas, E. Lopez-Aguilera, and D. Camps-Mur, "Dynamic sensitivity control of access points for IEEE 802.11ax," in *Proc. IEEE Int. Conf. Commun. (ICC)*, May 2016, pp. 1–7.

[20] J. A. Fuemmeler, N. H. Vaidya, and V. V. Veeravalli, "Selecting transmit powers and carrier sense thresholds in CSMA protocols for wireless ad hoc networks," in *Proc. 2nd Annu. Int. Workshop Wireless Internet WICON*, 2006, p. 15, doi: 10.1145/1234161.1234176.

[21] P. B. Oni and S. D. Blostein, "Optimized physical carrier sensing threshold in high density CSMA/CA networks," in *Proc. 29th Biennial Symp. Commun. (BSC)*, Jun. 2018, pp. 1–5.

[22] P. B. Oni and S. D. Blostein, "PCS threshold selection for spatial reuse in high density CSMA/CA MIMO wireless networks," *IEEE Access*, vol. 7, pp. 112470–112482, 2019.
[23] *NS-3 Network Simulator*. Accessed: Sep. 1, 2020. [Online]. Available: https://www.nsnam.org/
[24] G. Holland, N. Vaidya, and P. Bahl, "A rate-adaptive MAC protocol for multi-hop wireless networks," in *Proc. 7th Annu. Int. Conf. Mobile Comput. Netw. MobiCom*, 2001, pp. 236–251.
[25] L. Kriara and M. K. Marina, "SampleLite: A hybrid approach to 802.11n link adaptation," *ACM SIGCOMM Comput. Commun. Rev.*, vol. 45, no. 2, pp. 4–13, Apr. 2015.
[26] J. Zhang, K. Tan, J. Zhao, H. Wu, and Y. Zhang, "A practical SNR-guided rate adaptation," in *Proc. IEEE INFOCOM 27th Conf. Comput. Commun.*, Apr. 2008, pp. 2083–2091.
[27] A. Kamerman and L. Monteban, "WaveLAN-II: A high-performance wireless LAN for the unlicensed band," *Bell Labs Tech. J.*, vol. 2, no. 3, pp. 118–133, Aug. 2002.
[28] M. Lacage, M. H. Manshaei, and T. Turletti, "IEEE 802.11 rate adaptation: A practical approach," in *Proc. 7th ACM Int. Symp. Modeling, Anal. Simulation Wireless Mobile Syst.*, 2004, pp. 126–134.
[29] J. C. Bicket, "Bit-rate selection in wireless networks," Ph.D. dissertation, Dept. Elect. Eng. Comput. Sci., Massachusetts Inst. Technol., Cambridge, MA, USA, 2005.
[30] F. Fietkau and D. Smithies. (2010). *Minstrel HT: New Rate Control Module for 802.11 n*. [Online]. Available: https://lwn.net/Articles/376765/
[31] R. Combes, A. Proutiere, D. Yun, J. Ok, and Y. Yi, "Optimal rate sampling in 802.11 systems," in *Proc. IEEE INFOCOM Conf. Comput. Commun.*, Apr. 2014, pp. 2760–2767.
[32] R. Combes, J. Ok, A. Proutiere, D. Yun, and Y. Yi, "Optimal rate sampling in 802.11 systems: Theory, design, and implementation," *IEEE Trans. Mobile Comput.*, vol. 18, no. 5, pp. 1145–1158, May 2019.
[33] T. L. Lai and H. Robbins, "Asymptotically efficient adaptive allocation rules," *Adv. Appl. Math.*, vol. 6, no. 1, pp. 4–22, Mar. 1985.
[34] A. Garivier and O. Cappé, "The KL-UCB algorithm for bounded stochastic bandits and beyond," in *Proc. 24th Annu. Conf. Learn. Theory*, 2011, pp. 359–376.
[35] W. R. Thompson, "On the likelihood that one unknown probability exceeds another in view of the evidence of two samples," *Biometrika*, vol. 25, nos. 3–4, pp. 285–294, Dec. 1933.
[36] E. Kaufmann, N. Korda, and R. Munos, "Thompson sampling: An asymptotically optimal finite-time analysis," in *Proc. Int. Conf. Algorithmic Learn. Theory*. Lyon, France: Springer, 2012, pp. 199–213.
[37] S. Paladino, F. Trovò, M. Restelli, and N. Gatti, "Unimodal thompson sampling for graph-structured arms," in *Proc. 21st AAAI Conf. Artif. Intell.*, 2017, pp. 2457–2463.
[38] V. Saxena, J. E. Gonzalez, I. Stoica, H. Tullberg, and J. Jaldén, "Constrained thompson sampling for wireless link optimization," 2019, *arXiv:1902.11102*. [Online]. Available: http://arxiv.org/abs/1902.11102
[39] H. Gupta, A. Eryilmaz, and R. Srikant, "Low-complexity, low-regret link rate selection in rapidly-varying wireless channels," in *Proc. IEEE INFOCOM Conf. Comput. Commun.*, Apr. 2018, pp. 540–548.
[40] *The MadWifi Project*. Accessed: Sep. 1, 2020. [Online]. Available: http://madwifi-project.org/
[41] D. Russo, B. Van Roy, A. Kazerouni, I. Osband, and Z. Wen, "A tutorial on thompson sampling," 2017, *arXiv:1707.02038*. [Online]. Available: http://arxiv.org/abs/1707.02038
[42] P. Del Moral, "Nonlinear filtering: Interacting particle resolution," *Comp. Rendus de l'Académie des Sci. Ser. I Math.*, vol. 325, no. 6, pp. 653–658, Sep. 1997.
[43] G. Pei and T. R. Henderson. *Validation of OFDM Model in Ns-3*. Accessed: Sep. 1, 2020. [Online]. Available: http://www.nsnam.org/~pei/80211ofdm.pdf
[44] S. Merlin. *TGax Simulation Scenarios*. Accessed: Sep. 1, 2020. [Online]. Available: https://mentor.ieee.org/802.11/dcn/14/11-14-0980-16-00ax-simulation-sce%narios.docx

ALEXANDER KROTOV (Member, IEEE) received the M.Sc. degree from Moscow Physics and Technology Institute, Moscow, Russia, in 2016. He has been a Researcher with the Institute for Information Transmission Problems since 2014. He is currently a Researcher with the Wireless Network Laboratory, Institute for Information Transmission Problems, Russian Academy of Sciences. His current research includes analysis and simulation of wireless networks, developing MAC protocols. He has authored 15 technical journal and conference publications. He received the Best Cited Review Paper Award from Elsevier Computer Communications and Moscow Government Award for young researchers. He contributes to the development of the NS-3 network simulator. In particular, he successfully completed the Google Summer of Code 2017 program.

ANTON KIRYANOV received the B.S. and M.S. degrees from the Moscow Institute of Physics and Technology (State University), in 2011 and 2013, respectively, and the Ph.D. degree in telecommunications from the Institute for Information Transmission Problems, Russian Academy of Sciences (IITP RAS), in 2017. From 2014 to 2015, he was an IEEE 802.11 voting member and took part in the development of the upcoming IEEE 802.11ax amendment by contributing a number of proposals that were accepted by task group AX. He has authored over 15 papers published in international journals and conference proceedings. His major research interests are connected with Wi-Fi and cellular networks with the focus on channel access methods and radio resource management for quality of service provisioning. He was a recipient of the Best Paper Award at the International Symposium on Wireless Communication Systems in 2012. He participates in national and international projects and researches within the framework of joint research projects with the leading telecommunication companies.

EVGENY KHOROV (Senior Member, IEEE) is currently the Head of the Wireless Networks Laboratory, Institute for Information Transmission Problems, Russian Academy of Sciences. He has led dozens of national and international projects sponsored by academia funds and industry. Being a voting member of IEEE 802.11, he has contributed to the 802.11ax standard as well as to Real-Time Applications TIG with many proposals. He has authored more than 100 articles. His main research interests are related to 5G and beyond wireless systems, next-generation Wi-Fi, protocol design, and QoS-aware cross-layer optimization. He was a recipient of the Russian Government Award in Science, several Best Papers Awards, and the Scopus Award Russia 2018. In 2015, 2017, and 2018, Huawei RRC awarded him as the Best Cooperation Project Leader. He gives tutorials and participates in panels at large IEEE events. He chairs TPC of the IEEE GLOBECOM 2018 CA5GS Workshop and IEEE BLACKSEACOM 2019. He was awarded as the Editor of the Year 2020 of *Ad Hoc Networks*.